

# EXOCOMETS, MINOR BODIES AND RESONANT PHENOMENA IN DEBRIS DISKS

H. Beust<sup>1</sup>

**Abstract.** Debris disks constitute the visible part of young planetary system. Resonant processes are important in debris disks as a natural way to generate asymmetries that are furthermore transported away by radiation pressure affecting dust particles. Several kinds of resonant processes may be present in these disks. Examples of systems are given where different processes are suspected. Focus is given then on Mean-Motion resonances and on the  $\beta$  Pictoris disk in particular, where the presence of numerous star-grazing exocomets is strongly suspected. This system is known today to harbour two giant planets. This fact leads to a revision of the exocomet generating model via Mean-Motion resonances proposed earlier.

Keywords: Stars: circumstellar matter, Stars: planetary systems, Celestial mechanics, Planets and satellites: dynamical evolution and stability

## 1 Introduction

### 1.1 Debris disks

Dusty disks imaged around young main sequence stars are known today as debris disks. Dozens of such disks have been imaged today. Several characteristics suggest that they constitute the visible part of young planetary system. It is first clear now that the dust is short lived versus collisions and radiation pressure (Thébaud et al. 2003). This implies the presence of a reservoir of matter made of larger parent bodies. Hence a debris disk is basically a disks of planetesimals. All these disks exhibit departures from a pure axisymmetric shape: asymmetries, gaps, warps, spirals. . . . The presence of these structures are usually associated with the perturbing action of hidden planets. Such planets have been indeed detected in some of them :  $\beta$  Pictoris (Lacour et al. 2021), Fomalhaut (Kalas et al. 2005), HD106906 (Lagrange et al. 2016). . . . Debris disks also presumably contain small amounts of circumstellar gas.

Gravitation processes are mostly dominant in debris disks. Planets, but also stellar companions in multiple stellar systems, have a gravitational action on the population of planetesimals, which affects the subsequent population of dust particles, and eventually generates the asymmetries observed. These actions can be chaotic, secular or resonant. Radiative processes are also important, as radiation pressure affects the dynamics of small dust particles and circumstellar gas. Dust particles are mostly produced by parent bodies which do not feel any noticeable radiation pressure thanks to their size. Collisional processes are of course important too, as collisions among the population of planetesimals, as well as among the dust particles themselves, ensure the replenishment of the dust population, and thus the survival of debris disks (Thébaud et al. 2003).

### 1.2 Radiation pressure

At the time they are produced, dust particles share approximately the same velocity as their parent body. But they feel an intense radiation pressure that causes them to see a “lighter” star. Consequently, they immediately start to follow a much wider orbit that transports them far away from their production site (Augereau et al. 2001). The dust particle may even be ejected. All this contributes to the radial transport of asymmetries.

---

<sup>1</sup> Univ. Grenoble Alpes, CNRS, IPAG, 38000 Grenoble, France

## 2 Resonances in debris disks

Resonances constitute a major source of non axisymmetric features and radial transport in debris disks. Three kinds of resonances can affect planetesimals in debris disks: Kozai-Lidov, Mean-motion and secular resonances.

Kozai-Lidov resonance (Kozai 1962) is an angular momentum exchange process that occurs between orbits that are initially significantly mutually inclined (by more than  $40^\circ$ ). In this context, the orbit with the smaller angular momentum (usually the inner one) is subject to large amplitude eccentricity modulations that can drive it very close to  $e = 1$ . Meanwhile, the mutual inclination drops by several tens of degrees. As naturally affecting non-planar systems, this process often concerns multiple stellar systems (Smallwood et al. 2020; Lubow et al. 2015), but it can be found in planetary systems (Beust et al. 2012), where it can trigger star-grazers generation (Bailey et al. 1992).

A secular resonance occur when one of the secular precession frequencies of a minor body happen to match one of the fundamental frequencies of the planetary system. Secular resonances are usually weaker and have longer timescales. Conversely, in an evolving planetary system, they are able to rapidly move radially. Subsequently, they can excite eccentricities and inclinations in planetesimal population when sweeping the disk (Toliou et al. 2019; Baguet et al. 2019). They are also invoked to explain the formation of gaps at large distances in massive disks (Yelverton & Kennedy 2018; Sefilian et al. 2021).

## 3 Dynamics of minor bodies in Mean-Motion resonance

Mean-Motion resonances (hereafter MMRs) occur when bodies have orbital frequencies within a simple rational ratio. This is quite a frequent configuration. MMRs are self-sustaining structures. Resonant perturbations on trapped bodies actually work at keeping them trapped. They are consequently able to concentrate particles. However, in other configurations they are also able to trigger the formation of gaps and non-axisymmetric features in disks (Wyatt 2003; Kuchner & Holman 2003; Tabeshian & Wiegert 2016, 2017). More generally, MMRs excite eccentricities and inclinations in disks, with two major consequences: i/ they enhance collisional activity, ii/ they favour radial transport, leading to the generation star-grazers in extreme cases.

Consider the simple case of a small body orbiting a star, and trapped in a  $p + q:p$  MMR with a coplanar planet. Consider also the mean longitudes  $\lambda$  and  $\lambda'$  of the planetesimal and of the planet respectively as well as their longitudes or periastra ( $\varpi, \varpi'$ ). Let us introduce now the *critical resonant arguments*  $\sigma$  and  $\nu$  (Morbidelli & Moons 1993; Henrard & Caranicolas 1990) as

$$\sigma = \frac{p+q}{q} \lambda' - \frac{p}{q} \lambda - \varpi \quad \nu = -\frac{p+q}{q} \lambda' + \frac{p}{q} \lambda + \varpi' \quad . \quad (3.1)$$

It is worth noticing that  $\sigma$  and  $\nu$  are naturally slow varying quantities thanks to the MMR configuration. Physically,  $\sigma$  approximately represents the longitude of the fixed conjunction between both bodies with respect to the periastron of the small body. Integer  $|q|$  is the order the MMR, and represents the number of conjunction positions. The larger  $|q|$ , the weaker the resonance.

A secular treatment of the motion inside the MMR shows that trapped planetesimals are subject to coupled  $(\sigma, a, e)$  librations that act at maintaining the configuration. For any particle trapped in the MMR,  $\sigma$  remains constrained more or less close to an equilibrium value, depending on the amplitude of the resonant librations. As a consequence, both bodies (the planetesimal and the perturbing planet) never get too close to each other, even in the case of crossing orbits. This process is known as *phase protection mechanism*, and actually acts as protecting the small bodies from close encounters with the planet.

The  $\sigma$  libration is coupled with  $(a, e)$  librations. It turns out that eccentricities are maximum when  $\sigma$  is at equilibrium value, i.e., for specific constrained longitudes of periastron. The combination of these effects is the creation of  $p + q$  azimuthal clumps in the disks concentrating particles (Wyatt 2003; Kuchner & Holman 2003). However, numerical simulations by Reche et al. (2008) have shown that these clumps are very sensitive to the eccentricity of the perturbing planet. They rapidly get blurred with increasing planet eccentricity (Fig. 1).

However, MMRs are narrow structures in semi-major axis. Even if present, clumps are likely to remain invisible in the middle of a disk made of non-resonant bodies. But if the planet migrates even slowly, the MMR sweeps the disk and can capture more planetesimals, leading to an enhanced resonant population. Moreover, additional dust particles can get trapped into MMR thanks to Poynting-Robertson drag (Kuchner & Holman 2003; Deller & Maddison 2005). And in the case of planet-crossing disks, phase protection mechanism can help resonant particles to survive, but not non-resonant ones, leading to the depletion of non-resonant regions Pearce et al. (2021). These factors all contribute to render resonant clumps more visible.

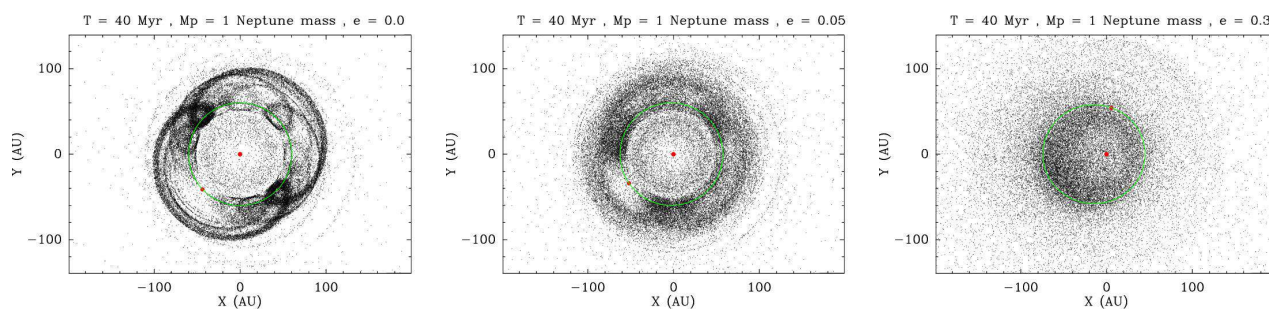


**Fig. 1.** Simulation of rings of particles trapped in various MMRs (2:3, 3:4) with a single planet, for increasing values of the planet eccentricity, from left to right (Reche et al. 2008). Resonant clumps are visible for  $e = 0$  but disappear as soon as the eccentricity is significant.

MMRs are also capable of triggering the generation of star-grazers out of a disk of planetesimals. This requires however the eccentricity of the planet to be non-zero. But even for values as small as  $e = 0.05$ , the eccentricity of particles trapped in some MMRs like 4:1, 3:1, and 5:2 may grow over a long time and reach very high values close to 1, thus generating star-grazers (Beust & Morbidelli 1996, 2000). This mechanism is even more efficient for larger planet eccentricity values (Pichierri et al. 2017).

#### 4 Application to specific systems

We come now to presenting a few examples of debris disks where these mechanism have been claimed to be active. Vega for instance is an A0 star surrounded by a large debris disk viewed pole-on at various wavelengths, but always appearing with non-axisymmetric clumpy structures (Wyatt 2003; Marsh et al. 2006). This asymmetry was interpreted and modeled as resonant clumps arising mainly from a 2:3 MMR with a Neptune sized planet orbiting the star at  $\sim 65$  au (Wyatt 2003). More recently, Zheng et al. (2017) presented an alternative model involving a secular resonance with a migrating planet. This model is actually close to that of Sefilian et al. (2021). However, in the case of Vega, no planet has been detected so far. Conversely,  $\epsilon$  Eridani is another example of system where resonant clumps have been invoked to explain observations, but a Jupiter-sized planet was actually discovered there (Mawet et al. 2019).

Fomalhaut is another interesting example of system where MMRs could play a significant role. A nice eccentric ( $\sim 0.1$  ellipticity) dust ring was imaged with HST at  $\sim 140$  au from this star. Furthermore, a planet was imaged right inside the ring, suggesting a shepherding role with respect to it (Kalas et al. 2005). From photometric estimates, this planet appeared in any case to be significantly smaller than Jupiter. Then, its orbital motion was detected despite a large orbital period. As of yet, 9 astrometric positions since 2004 have been recorded (Gaspar & Rieke 2020). This allowed to perform an orbital fit revealing a highly eccentric orbit ( $e \gtrsim 0.8$ ) that appears to cross the disk (Kalas et al. 2013; Beust et al. 2014). Does it mean that we are viewing an unstable configuration? Pearce et al. (2021) show that this is not obvious, as the disk could in fact be in MMR configuration with the planet. Another puzzling issue is the origin of this planet. It could actually have been sent there after a resonant (5:2) interaction with another, more massive planet orbiting inside (the real shepherd of the disk) that still needs to be discovered (Chiang et al. 2009; Faramaz et al. 2015).

PDS 70 is a very young system where two still accreting planets (named PDS 70 b and c) have been detected orbiting the star at  $\sim 20$  au and  $\sim 33$  au. These planets are presumably locked in a 2:1 MMR configuration. The 2-planet system is surrounded by a circumstellar outer disk, with accretion streams on the outer planet (Müller et al. 2018; Keppler et al. 2019; Wang et al. 2021). Such features are compatible with a dynamical disk-planet interaction process (Toci et al. 2020)

#### 5 Gas in the $\beta$ Pictoris disk

Gas in the circumstellar disk of  $\beta$  Pic was detected very early in the stellar spectrum (Hobbs et al. 1985), thanks to the edge-on orientation of the disk. This gas appears to be in Keplerian motion around the star, despite a strong radiation pressure from the star. However Fernández et al. (2006); Roberge et al. (2006); Brandeker (2011) showed that the abundance of Carbon can render the whole gas self-braking. This gas cannot be primordial

because of radiation pressure. It must be continuously replenished from a inner reservoir, by evaporating planetesimals Lagrange et al. (1998), or by grain-grain collisions or photodesorption Kral et al. (2015). Apart from stable components, repeated observations of various metallic species (Ca II, Mg II, Al III Vidal-Madjar et al. 1994) have revealed frequent and transient additional absorption components, most of the time redshifted by tens to hundreds of km/s with respect to the stellar velocity, with variation time-scales of a few days or even less (Ferlet et al. 1987; Lagrange-Henri et al. 1992; Petterson & Tobin 1999; Kennedy 2018; Tobin et al. 2019). These events have been convincingly modeled as resulting from the sublimation of star-grazing exocomets in the vicinity of the star (Beust et al. 1990, 1996; Crawford et al. 1998). This scenario has been termed 'Falling Evaporating Bodies' (FEBs), and it implies an activity of hundreds of such FEBs per year. The dynamical origin of these star-grazers is putatively related to planetary perturbations. The Kozai-Lidov resonance, often presented as a source of star-grazers in the Solar System (Bailey et al. 1992), cannot be invoked here because of its natural rotational invariance. In this context, there should be as numerous redshifted as blueshifted events. MMRs represent conversely a potential anisotropic source of FEBs (Beust & Morbidelli 1996). This model is indeed able to efficiently trigger the FEB phenomenon and reproduce nearly all their characteristics, provided the planet assumes an eccentricity  $e \gtrsim 0.05$ , and has a suitable value  $\varpi = -70^\circ \pm 20^\circ$  of longitude of periastron with respect to the line of sight. Detailed modeling (Beust & Morbidelli 2000; Thébault & Beust 2001) came to the conclusion that the planet was presumably orbiting the star at  $\sim 10$  au.

Such a planet, referred today to as  $\beta$  Pic b, was indeed detected in high contrast imaging (Lagrange et al. 2010; Wang et al. 2016; Lagrange et al. 2019a). It is tempting to identify it with the previously suspected planet. A regular astrometric follow-up of  $\beta$  Pic b (Chauvin et al. 2012; Wang et al. 2016; Lagrange et al. 2019a) helps specifying its orbit. As of yet, the planet's semi-major axis is close to 9 au and has moderate eccentricity. The mass of  $\beta$  Pic b is less easy to constrain. Based on joint analysis of *Gaia* and *Hipparcos* data, Snellen & Brown (2018) report a mass of  $11 \pm 2 M_{\text{Jup}}$ , while Dupuy et al. (2019) derives  $13.1^{+2.8}_{-3.2} M_{\text{Jup}}$ .

These characteristics were highly compatible with the putative planet of the FEB model. Meanwhile, analysis of the radial velocity data of the star (Lagrange et al. 2019b), combined with observations by the GRAVITY interferometer (Nowak et al. 2020), led to the identification of another massive planet termed  $\beta$  Pic c orbiting the star at 2.7 au. All orbital determinations aim now at fitting both planetary orbits together (Lagrange et al. 2020; Nowak et al. 2020; Lacour et al. 2021). As of yet,  $\beta$  Pic c appears slightly less massive ( $\sim 8 M_{\text{Jup}}$ ) than  $\beta$  Pic b but significantly more eccentric, with an eccentricity around 0.3.

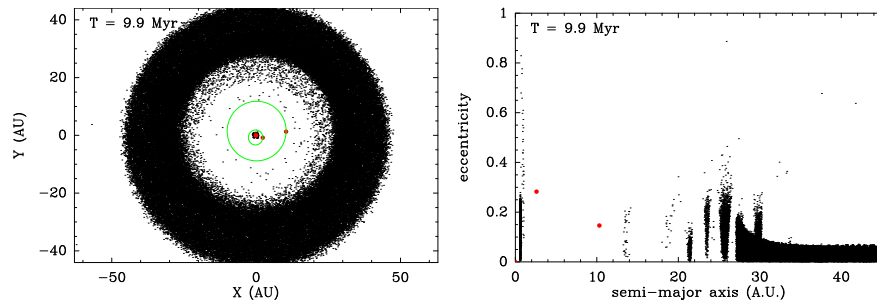


**Fig. 2.** Outcome after a 10 Myr simulation of a disk of planetesimals initially between 0.5 au and 45 au in the environment of  $\beta$  Pic b and  $\beta$  Pic c, viewed from above (left), and displayed in (semi-major axis, eccentricity) space (right). The red bullets show the location of the planets and the star, and the black dots stand for the remaining planetesimals.

The presence of  $\beta$  Pic c complicates the FEB picture. FEB progenitors trapped in an inner MMR with  $\beta$  Pic b orbits initially outside  $\beta$  Pic c's orbit. During the resonant eccentricity increase process that drives them to the FEB state, they come to regularly cross that orbit. Subsequent close encounters with  $\beta$  Pic c could eject it well before reaching the FEB state. Beust et al. (2022, in prep.) present new dynamical simulations involving a disk of planetesimals in the presence of both planets. They first show that the whole disk between  $\sim 1$  au and  $\sim 20$  au is unstable versus perturbations by the planets (Fig. 2). Hence FEBs cannot originate from that region. In Fig. 2 however, a small ring of particles survives inner to  $\beta$  Pic c's orbit. Fig. 3 focuses on this inner ring. The disk appears severely carved down to  $\sim 0.7$  au by perturbations by  $\beta$  Pic c. But up to  $\sim 1$  au, many disk particles are still present after 20 Myr and reach high eccentricity values, thus becoming FEB candidates. The eccentricity increase is preferably done at specific semi-major axis values corresponding to inner MMRs with  $\beta$  Pic c. The process is highly active at  $t = 2$  Myr but it is still present at  $t = 20$  Myr.

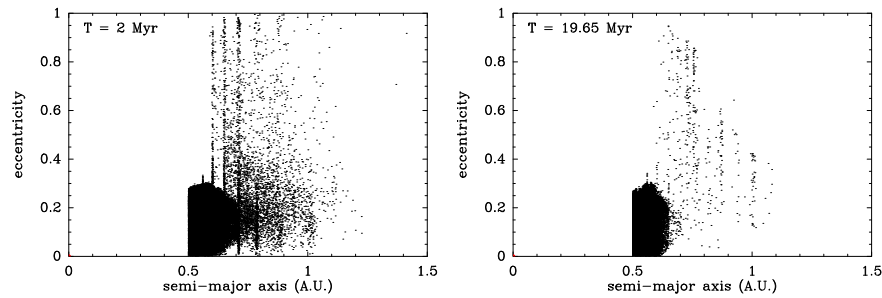


**Fig. 3.** Outcome in  $(a, e)$  space of a disk of planetesimals initially between 0.5 au and 1.5 au, in the same conditions as in Fig. 2, after 2 Myr (left) and 20 Myr (right). Both planets are outside the panel.

A new picture of the FEB generation mechanism arises. MMRs are still the preferred route, as contrary to Kozai resonance, they trigger an asymmetric infall (Beust & Morbidelli 1996, 2000; Thébault & Beust 2001) that better matches the observational statistics (Beust et al. 1996). MMRs with a single giant planet similar to  $\beta$  Pic b were previously invoked, with FEB progenitors starting around 4–5 au. We are now considering planetesimals trapped in higher order (7:1, 8:1...) MMRs with  $\beta$  Pic c, starting from a much inner region. The picture is even more complex. Following individually the evolution of various particles, Beust et al. (2022, in prep.) show that they undergo a gradual semi-major axis increase before getting trapped into MMRs with  $\beta$  Pic c. This is due to non-secular perturbations from  $\beta$  Pic c, and is enhanced by the outer presence of  $\beta$  Pic b. The fact that planetesimals may spend a significant time in the disk before being captured into a MMR explains the duration of the mechanism. Thébault & Beust (2001) had shown that in the previous model with only  $\beta$  Pic b, the 4:1 and 3:1 MMRs with  $\beta$  Pic b quite rapidly cleared out, causing the FEB process to nearly stop after 1–2 Myrs. Here the non-secular semi-major axis drift combined with the enhanced efficiency of the resonant capture process helps new planetesimals to continuously enter the MMRs under consideration and sustain the FEB activity over more than 20 Myrs.

## 6 Conclusions

Debris disks are the visible part (dust) of young planetary systems. Resonant processes in these systems are a major source of evolution: generation of asymmetries, excitation of eccentricities and inclinations, radial transport (inwards outwards). Each debris disk / young system has its own history and characteristics and must be the subject of a dedicated study.  $\beta$  Pictoris is the historical prototype of debris disk, associated with a planetary system holding at least two giant planets. Falling Evaporating Bodies in the  $\beta$  Pic system is an example of extreme resonant radial transport. The presence of planets  $\beta$  Pic b and  $\beta$  Pic c complicates the initial model initially built with one single planet. Actually MMRs with  $\beta$  Pic c now seem better suited to act as a dynamical source of FEBs, enhanced by the distant perturbing action of  $\beta$  Pic b.

All (or most of) the computations presented in this paper were performed using the GRICAD infrastructure (<https://gricad.univ-grenoble-alpes.fr>), which is supported by Grenoble research communities.

## References

- Augereau, J. C., Nelson, R. P., Lagrange, A. M., Papaloizou, J. C. B., & Mouillet, D. 2001, *A&A*, 370, 447
- Baguet, D., Morbidelli, A., & Petit, J. M. 2019, *Icarus*, 334, 99
- Bailey, M. E., Chambers, J. E., & Hahn, G. 1992, *A&A*, 257, 315
- Beust, H., Augereau, J. C., Bonsor, A., et al. 2014, *A&A*, 561, A43
- Beust, H., Bonfils, X., Montagnier, G., Delfosse, X., & Forveille, T. 2012, *A&A*, 545, A88
- Beust, H., Lagrange, A. M., Plazy, F., & Mouillet, D. 1996, *A&A*, 310, 181
- Beust, H., Lagrange-Henri, A. M., Vidal-Madjar, A., & Ferlet, R. 1990, *A&A*, 236, 202
- Beust, H. & Morbidelli, A. 1996, *Icarus*, 120, 358
- Beust, H. & Morbidelli, A. 2000, *Icarus*, 143, 170
- Brandeker, A. 2011, *ApJ*, 729, 122

- Chauvin, G., Lagrange, A. M., Beust, H., et al. 2012, *A&A*, 542, A41
- Chiang, E., Kite, E., Kalas, P., Graham, J. R., & Clampin, M. 2009, *ApJ*, 693, 734
- Crawford, I. A., Beust, H., & Lagrange, A. M. 1998, *MNRAS*, 294, L31
- Deller, A. T. & Maddison, S. T. 2005, *ApJ*, 625, 398
- Dupuy, T. J., Brandt, T. D., Kratter, K. M., & Bowler, B. P. 2019, *ApJ*, 871, L4
- Faramaz, V., Beust, H., Augereau, J. C., Kalas, P., & Graham, J. R. 2015, *A&A*, 573, A87
- Ferlet, R., Hobbs, L. M., & Vidal-Madjar, A. 1987, *A&A*, 185, 267
- Fernández, R., Brandeker, A., & Wu, Y. 2006, *ApJ*, 643, 509
- Gaspar, A. & Rieke, G. 2020, *Proceedings of the National Academy of Science*, 117, 9712
- Henrard, J. & Caranicolas, N. D. 1990, *Celestial Mechanics and Dynamical Astronomy*, 47, 99
- Hobbs, L. M., Vidal-Madjar, A., Ferlet, R., Albert, C. E., & Gry, C. 1985, *ApJ*, 293, L29
- Kalas, P., Graham, J. R., & Clampin, M. 2005, *Nature*, 435, 1067
- Kalas, P., Graham, J. R., Fitzgerald, M. P., & Clampin, M. 2013, *ApJ*, 775, 56
- Kennedy, G. M. 2018, *MNRAS*, 479, 1997
- Keppler, M., Teague, R., Bae, J., et al. 2019, *A&A*, 625, A118
- Kozai, Y. 1962, *AJ*, 67, 591
- Kral, Q., Thébault, P., Augereau, J. C., Boccaletti, A., & Charnoz, S. 2015, *A&A*, 573, A39
- Kuchner, M. J. & Holman, M. J. 2003, *ApJ*, 588, 1110
- Lacour, S., Wang, J. J., Rodet, L., et al. 2021, *A&A*, 654, L2
- Lagrange, A. M., Beust, H., Mouillet, D., et al. 1998, *A&A*, 330, 1091
- Lagrange, A. M., Boccaletti, A., Langlois, M., et al. 2019a, *A&A*, 621, L8
- Lagrange, A. M., Bonnefoy, M., Chauvin, G., et al. 2010, *Science*, 329, 57
- Lagrange, A. M., Langlois, M., Gratton, R., et al. 2016, *A&A*, 586, L8
- Lagrange, A. M., Meunier, N., Rubini, P., et al. 2019b, *Nature Astronomy*, 3, 1135
- Lagrange, A. M., Rubini, P., Nowak, M., et al. 2020, *A&A*, 642, A18
- Lagrange-Henri, A. M., Gosset, E., Beust, H., Ferlet, R., & Vidal-Madjar, A. 1992, *A&A*, 264, 637
- Lubow, S. H., Fu, W., & Martin, R. G. 2015, in *American Astronomical Society Meeting Abstracts*, Vol. 225, American Astronomical Society Meeting Abstracts #225, 330.07
- Marsh, K. A., Dowell, C. D., Velusamy, T., Grogan, K., & Beichman, C. A. 2006, *ApJ*, 646, L77
- Mawet, D., Hirsch, L., Lee, E. J., et al. 2019, *AJ*, 157, 33
- Morbidelli, A. & Moons, M. 1993, *Icarus*, 102, 316
- Müller, A., Keppler, M., Henning, T., et al. 2018, *A&A*, 617, L2
- Nowak, M., Lacour, S., Lagrange, A. M., et al. 2020, *A&A*, 642, L2
- Pearce, T. D., Beust, H., Faramaz, V., et al. 2021, *MNRAS*, 503, 4767
- Pettersson, O. K. L. & Tobin, W. 1999, *MNRAS*, 304, 733
- Pichierri, G., Morbidelli, A., & Lai, D. 2017, *A&A*, 605, A23
- Reche, R., Beust, H., Augereau, J. C., & Absil, O. 2008, *A&A*, 480, 551
- Roberge, A., Feldman, P. D., Weinberger, A. J., Deleuil, M., & Bouret, J.-C. 2006, *Nature*, 441, 724
- Sefilian, A. A., Rafikov, R. R., & Wyatt, M. C. 2021, *ApJ*, 910, 13
- Smallwood, J. L., Franchini, A., Chen, C., et al. 2020, *MNRAS*, 494, 487
- Snellen, I. A. G. & Brown, A. G. A. 2018, *Nature Astronomy*, 2, 883
- Tabeshian, M. & Wiegert, P. A. 2016, *ApJ*, 818, 159
- Tabeshian, M. & Wiegert, P. A. 2017, *ApJ*, 847, 24
- Thébault, P., Augereau, J. C., & Beust, H. 2003, *A&A*, 408, 775
- Thébault, P. & Beust, H. 2001, *A&A*, 376, 621
- Tobin, W., Barnes, S. I., Persson, S., & Pollard, K. R. 2019, *MNRAS*, 489, 574
- Toci, C., Lodato, G., Christiaens, V., et al. 2020, *MNRAS*, 499, 2015
- Toliou, A., Tsiganis, K., & Tsirvoulis, G. 2019, *Celestial Mechanics and Dynamical Astronomy*, 132, 1
- Vidal-Madjar, A., Lagrange-Henri, A. M., Feldman, P. D., et al. 1994, *A&A*, 290, 245
- Wang, J. J., Graham, J. R., Pueyo, L., et al. 2016, *AJ*, 152, 97
- Wang, J. J., Vigan, A., Lacour, S., et al. 2021, *AJ*, 161, 148
- Wyatt, M. C. 2003, *ApJ*, 598, 1321
- Yelverton, B. & Kennedy, G. M. 2018, *MNRAS*, 479, 2673
- Zheng, X., Lin, D. N. C., Kouwenhoven, M. B. N., Mao, S., & Zhang, X. 2017, *ApJ*, 849, 98